# Short-Period Kinetic Energy Cycles in the Atmosphere[1,2]

SU-TZAI SOONG AND ERNEST C. KUNG

*Dept. of Atmospheric Science, University of Missouri, Columbia*

(Manuscript received 18 March 1969)

ABSTRACT

Short-period cycles in the large-scale atmospheric circulation were investigated with time series of kinetic energy, its generation and outflow, which were computed twice a day for a 5-year period over the North American Continent. The spectra were computed from the autocorrelation curves, and were compared with the red noise spectra to evaluate the statistical significance of the energy cycles.

The maxima of time spectra of different energy parameters show frequent agreement. The commonly reported kinetic energy cycles with periods of one to two weeks are observed; however, they are not statistically significant and also show very high year-to-year irregularity. Significant cycles with periods around 40 days and 2–4 days are also noted.

## 1. Introduction

Time variations of energy parameters are beginning to receive increasing attention with the progress of general circulation research and numerical weather prediction.

The seasonal variation is a regular long-period cycle ultimately in response to the annual variation of the incident solar energy. Preceeding this investigation, Kung and Soong (1969) studied the seasonal variation of kinetic energy, its generation, transport, and dissipation over the North American Continent for a 5-year period. In their study the basic annual cycles and an additional important half-year cycle were described with the aid of Fourier analysis and its variance spectrum.

With regard to short-period cycles, both laboratory experiments (Fultz *et al.*, 1959) and numerical experiment (Lorenz, 1963) show that the oscillation of circulation proceeds regularly and periodically when the rotation rate of the simulated earth is moderate. As the rate of rotation increases, an irregular variation is superposed on the traveling waves. Hence, it is conceivable that the evolution of the atmospheric circulation possesses short-period cycles as well as random variations.

The reported observations of the short-period energy cycle both with real atmospheric data and comprehensive numerical models of the atmosphere are far from conclusive. This is because the nature of the short-period oscillation is not as obvious as that of the seasonal variation, and it is difficult to apply a proper statistical method for analysis. Shapiro and Ward (1960) have computed the time-space spectrum of the geostrophic meridional kinetic energy at the 500-mb level. They concluded that there were no preferred periods of oscillation except the annual cycle. However, Smagorinsky's (1963) two-level numerical simulation model of the general circulation showed that the kinetic energy and the conversion terms had cycles of 11–12 days. The nine-level general circulation model of Smagorinsky *et al.* (1965) showed irregular cycles of about two weeks. Kung (1966) has indicated that the behavior of kinetic energy generation and outflow over the North American Continent has a cyclic appearance with a period of the order of 10 days.

In an attempt to examine the statistical significance of short-period kinetic energy cycles, a method of time spectrum analysis was applied to the vertically integrated daily kinetic energy parameters over the North American Continent for 0000 and 1200 GMT observations during a 5-year period in this study. The significance of the maxima of each time spectrum was then tested at the 1% and 5% levels.

## 2. Data and method of analysis

Using wind and geopotential observations at 0000 and 1200 GMT over the North American Continent from the MIT General Circulation Data Library (prepared under National Science Foundation Grants GP 820 and GP 3657), Kung (1967) has estimated the long-period budget of the kinetic energy and terms in the kinetic energy equations at 0000 and 1200 GMT for a 5-year period from May 1958 through April 1963. The vertically integrated energy parameters from the surface to 100 mb for each daily observation in his original computation were the data source of this

[1] Research supported by the Atmospheric Science Section, National Science Foundation, under Grant GA-1287.

[2] Contribution from the Missouri Agricultural Experiment Station: Journal Series No. 5648.

study. The energy parameters investigated in this study include the following:

| | |
|---|---|
| $k=(\frac{1}{2})\overline{\mathbf{V}\cdot\mathbf{V}}$ | kinetic energy |
| $-\overline{\mathbf{V}\cdot\nabla\phi}$ | kinetic energy generation |
| $(1/A)\oint_c k\mathbf{V}\cdot\mathbf{n}ds$ | horizontal transport of the kinetic energy out of the continent or kinetic energy outflow. |

In the above $\mathbf{V}$ is the horizontal wind velocity, $\phi$ the geopotential, $s$ the boundary of the continental region, $\mathbf{n}$ the outward-directed unit vector normal to the continental boundary, $A$ the area of the continental region, and $\nabla$ the isobaric del operator. The horizontal upper bar denotes the area mean of a parameter over the continent. These are the parameters which were computed independently and directly from the atmospheric data.

In the original computation by Kung (1967), the kinetic energy parameters for January and September 1959, and April 1962, were not calculated for the 1200 GMT observations due to technical difficulty with the original data tape. Some days were eliminated in other months because the number of the available stations was not sufficient for analysis. Hence, the kinetic energy parameters on hand for this study cover a 5-year period with some missing data. The total number of days available for analysis was 1747 days for the 0000 GMT observation and 1646 days for the 1200 GMT observation.

As we are investigating short-period cycles whose regularity is not certain, a time-spectrum analysis which applies a type of harmonic analysis to the autocorrelation function was used.

Kung and Soong (1969) have shown that all of the three kinetic energy parameters concerned have clear regular cycles of a 1-year period, and that the kinetic energy generation $-\overline{\mathbf{V}\cdot\nabla\phi}$ and outflow $(1/A)\oint_c k\mathbf{V}\cdot\mathbf{n}ds$ have additional regular cycles of a half-year period. As a result "pre-whitening" is needed to remove all these known exact periodicities that would otherwise dominate the spectrum and might impair its fidelity at other frequencies. Thus, both the one-year and half-year cycles of $-\overline{\mathbf{V}\cdot\nabla\phi}$ and $(1/A)\oint_c k\mathbf{V}\cdot\mathbf{n}ds$ were filtered out by subtracting them from the original time series. However, for the kinetic energy level $\bar{k}$, only the one-year cycle was removed because of the insignificance of the half-year cycle.

Following the procedure described by Panofsky and Brier (1965), if we are given a series of variables $X_1\cdots X_i\cdots X_N$ at equal time intervals, the autocorrelation of lag $L$ is calculated from:

$$r_L'=\sum_{i=0}^{N-L}(X_i-\bar{X})(X_{i+L}-\bar{X})/(ns_X^2), \tag{1}$$

where $L$ is the number of days of lag from 0 to $M$, $n$ the number of pairs of $X$ used in the calculation, and $s_X$ the standard deviation of the variable $X$. The wave notation indicates the time mean. When we have a long time series of data, the equation can be simplified to

$$r_L'=\widetilde{(X_iX_{i+L}-\bar{X}^2)}/s_X^2, \tag{2}$$

without losing any appreciable degree of accuracy.

According to the above equations, each increase in lag $L$ decreases the number of pairs of data available. Hence, in a random series, the value of $r_L'$ tends to increase with an increase of $L$. Alter (1933) made a correction for this by dividing each autocorrelation by the standard deviation of $r_L'$ which in a random series is approximately equal to $(N-L-1)^{-\frac{1}{2}}$, where $N$ is the number of data available in each time series. This correction was accepted by Brooks and Carruthers (1953). We adopted and modified this correction scheme to cope with this problem as well as the problem of missing data.

In handling the problem of missing data, due to rather fast oscillation of $-\overline{\mathbf{V}\cdot\nabla\phi}$ and $(1/A)\oint_c k\mathbf{V}\cdot\mathbf{n}ds$, usual interpolation schemes do not fit well; thus, instead of interpolation, missing data are ignored. Hence, by modifying Alter's approach the autocorrelation $r_L$ is calculated as

$$r_L=r_L'(n-1)^{\frac{1}{2}}/(N-1)^{\frac{1}{2}}, \tag{3}$$

where $n$ is the number of effective pairs of data in which neither $X_i$ nor $X_{i+L}$ is missing. The purpose of multiplying by $(N-1)^{-\frac{1}{2}}$ is to make $r_L=r_L'$ when $L=0$. It should be noted that in this study $N$ is the number of data available in the time series where missing data are ignored.

The amplitude of the $i$th harmonic in the Fourier analysis of the autocorrelation for lags from 0 to $M$ is given by

$$B_i=r_0/M+(2/M)\sum_{L=1}^{M-1}[r_L\cos(\pi iL/M)]+(r_M/M)(-1)^i, \tag{4}$$

where in the case of $B_0$ and $B_M$, the amplitudes resulting from this formula have to be divided by 2. The time spectrum derived by the above equation is the fractional variance spectrum, since $r_L$ is an even function, equal to one when $L$ equals zero. The fundamental period is $2M$ and the relation between the frequency and period is period$=2M/$frequency. The amplitude $S_i$ in the smoothed time spectrum may be derived by the weighted running mean forming the smoothed estimation for the $i$th harmonic, given by

$$S_i=0.25B_{i-1}+0.50B_i+0.25B_{i+1}, \tag{5}$$

except for $i=1$ and $i=M$. For $S_1$ and $S_M$, one is

TABLE 1. Estimated $\rho$ for $\bar{k}$, $-\overline{\nabla\cdot\nabla\phi}$ and $(1/A)\oint_c k\mathbf{V}\cdot\mathbf{n}ds$. The values in parentheses indicate the one-lag autocorrelations.

| Time (GMT) | $\bar{k}$ | $-\overline{\nabla\cdot\nabla\phi}$ | $(1/A)\oint_c k\mathbf{V}\cdot\mathbf{n}ds$ |
|---|---|---|---|
| 0000 | 0.75 (0.76) | 0.30 (0.30) | 0.38 (0.38) |
| 1200 | 0.76 (0.78) | 0.28 (0.29) | 0.42 (0.43) |

weighted 75% and the adjacent one 25%, thus leaving the summation of $S_i$ still equal to one.

When a time series possesses only a certain degree of persistence with random variations, its spectrum will be a general suppression of fractional variance at higher frequencies and consequent inflation at lower frequencies. Its population spectrum is a "red noise spectrum," which can be estimated, as done by Gilman *et al.* (1963), by

$$S_i' = (1-\rho^2)/[1-2\rho\cos(\pi i/M)+\rho^2], \qquad (6)$$

where $\rho$ is the one-lag autocorrelation of the time series consisting only of red noise, and $\rho$ measures the degree

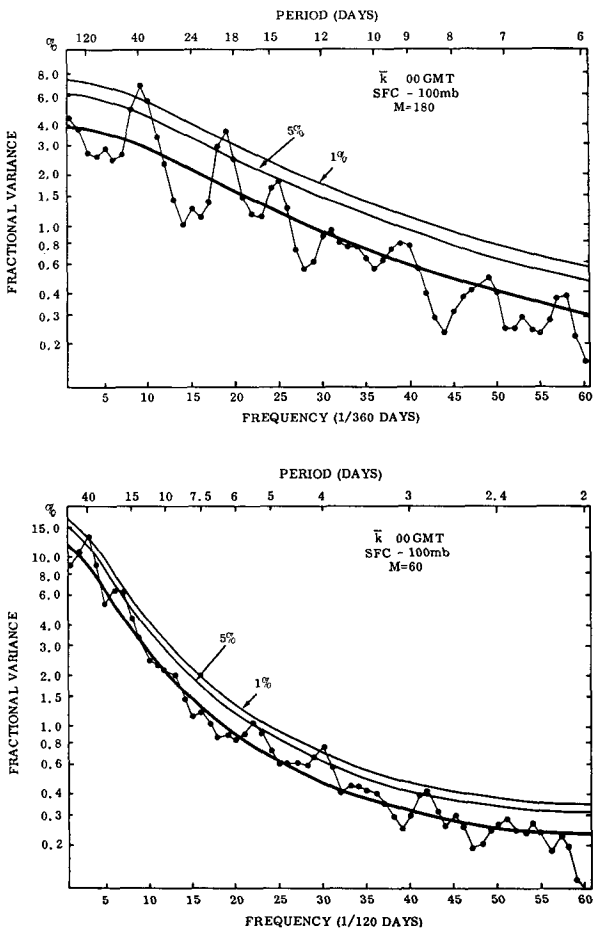


FIG. 1. Time spectra of kinetic energy $\bar{k}$ at 0000 GMT. The broad curve is the estimated red noise spectrum while the thin curves are the 5% and 1% significance levels.

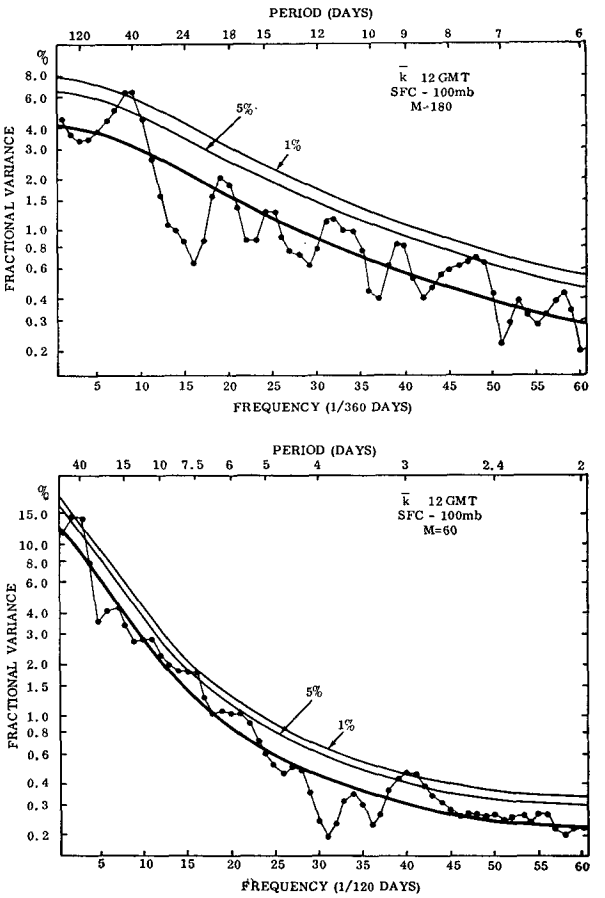


FIG. 2. Same as Fig. 1 except for 1200 GMT.

of persistance. If a real-time series contains any regular time cycle, estimates of $\rho$ from the one-lag autocorrelation are no longer warranted. In this case, $\rho$ may be evaluated by comparing the estimated spectrum with a family of red noise curves of different degrees of persistence using the iterative least-square procedure for selecting the proper red noise spectrum. Here, the logarithmic scale is used in the ordinate to give about equal weight to fluctuations of the fractional variance from high to low frequencies. The values of estimated $\rho$ are shown in Table 1 as well as the one-lag autocorrelation for three kinetic energy parameters. It should be noted that there is good agreement between the $\rho$ thus estimated and the one-lag autocorrelation, the difference between them being no more than 0.02.

With a null hypothesis that the time spectra of kinetic energy parameters are due to persistence only, i.e., they are not different from the red noise spectrum, the significance tests at the 5% and 1% levels are applied to the computed spectra to see if there are any important cycles. The 5% and 1% equal significance lines are derived by multiplying the red noise spectrum with the 5% and 1% chi-square limits divided by the degrees of freedom (see Blackman and Tukey, 1958).

The number of degrees of freedom in this case is $(2N-M/2)/M$.

## 3. Results of analysis

The time spectra of kinetic energy $\bar{k}$, generation $-\overline{\mathbf{V}\cdot\nabla\phi}$ and outflow $(1/A)\oint_c k\mathbf{V}\cdot\mathbf{n}ds$ at 0000 and 1200 GMT observations are separately presented in Figs. 1–6 so as not to include diurnal oscillations. The ordinate in each figure is the fractional variance at each frequency. As we pointed out, the intervals between the red noise spectrum and the 5% or 1% equal significance lines are proportional to the fractional variance of the red noise spectrum at that frequency. Since the red noise spectrum diminishes gradually from lower frequencies (longer periods) to higher frequencies (shorter periods), the red noise spectrum and both of the equal significance lines tend to converge with increasing frequencies. For the purpose of examining the significance at higher frequencies, a logarithmic scale is used for the ordinate to make the distance between the red noise spectrum and the equal significance lines almost the same throughout all frequencies with which we are concerned. For ease in comparing the length of periods with respect to corresponding frequencies, the periods in days are added at the top of each figure. The upper halves of these figures are the time spectra of the kinetic energy parameters derived from the Fourier analysis of the autocorrelation truncated at lag $M=180$ days. These spectra have a higher resolution (see Griffith *et al.*, 1956; Ward and Shapiro, 1961). In these spectra, the frequency ranges from 1 to 180, and the corresponding period from 360 to 2 days. Since the periods from 6–2 days are distributed over 120 frequencies from 61–180, the time spectrum is flattened in this portion, and it is difficult to see the important short periods. Thus, since only the first 60 frequencies are presented in the upper halves of those figures, the shortest period presented is 6 days. Periods of 6–2 days, as well as some other longer periods, are presented in the lower halves of the figures which are the time spectra calculated from autocorrelations of the same kinetic energy parameters at the same time of observation but truncated at lag $M=60$ days. These time spectra have a lower resolution; the frequency ranges from 1 to 60 and the period from 120 to 2 days. We shall use $F$ to denote the frequency of a higher resolution spectrum and $f$ that of a lower resolution spectrum.

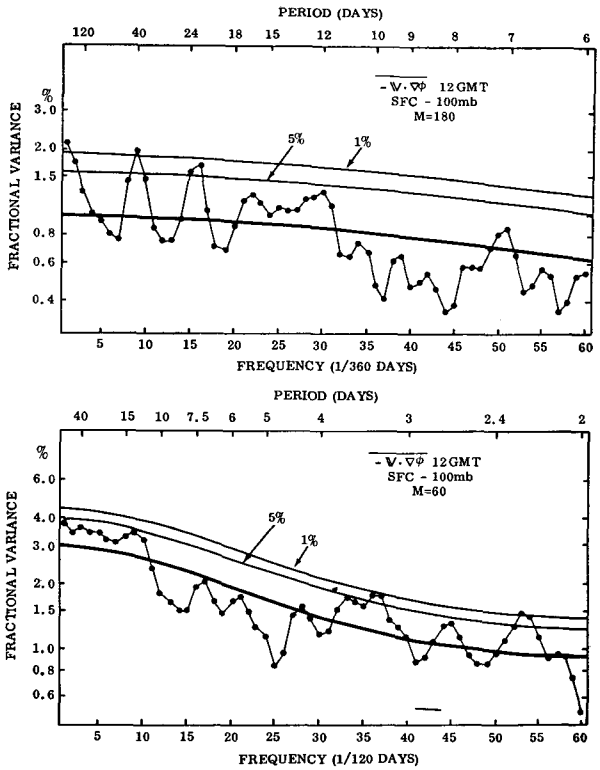


FIG. 4. Same as Fig. 3 except for 1200 GMT.

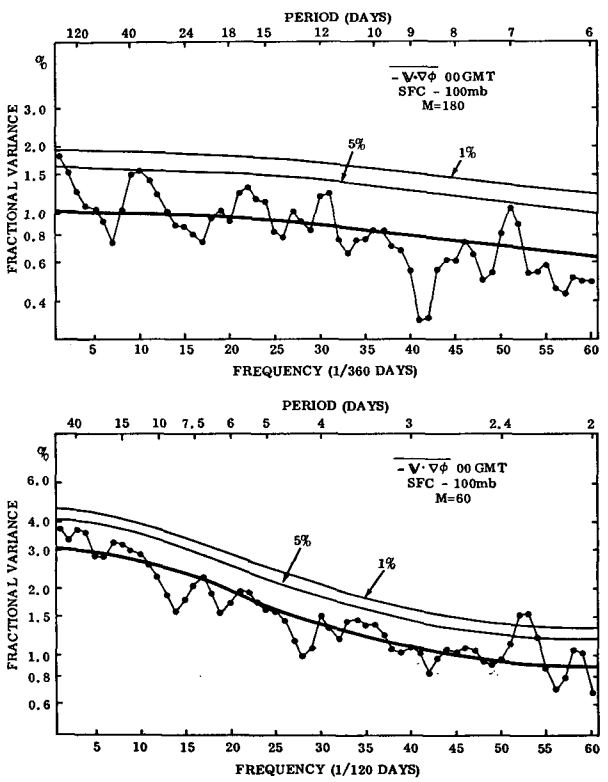


FIG. 3. Time spectra of kinetic energy generation $-\overline{\mathbf{V}\cdot\nabla\phi}$ at 0000 GMT. See legend of Fig. 1 for description of curves.

Fig. 1 depicts the time spectra of $\bar{k}$ at 0000 GMT. The periods of 40 days ($F=9$) and 19 days ($F=19$) are very distinct in the high resolution time spectrum. Both of them exceed the 1% significance level. Other frequencies also have some maxima; however, they are not statistically significant. The low resolution time spectrum shows the same trend in the region of lower frequencies as that in those of high resolution. It has another important period of 4 days ($f=30$). The

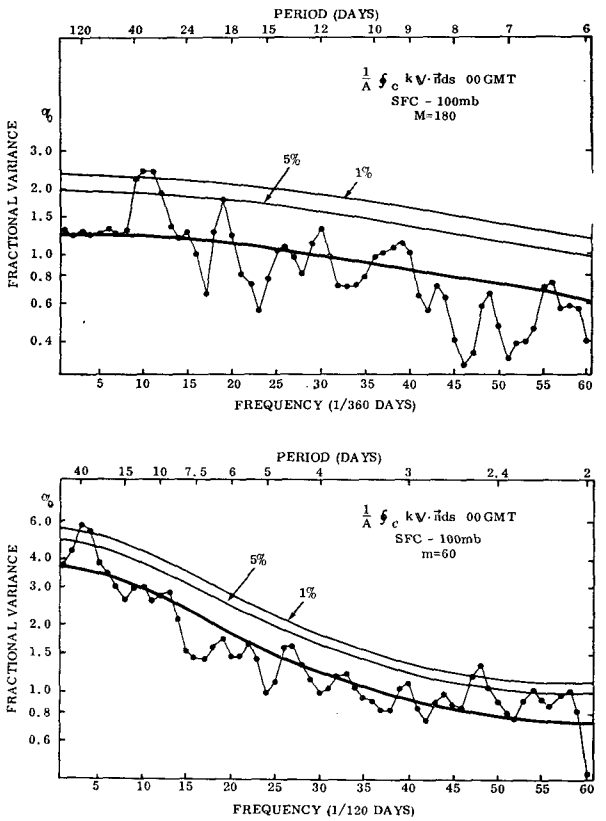


FIG. 5. Time spectra of kinetic energy outflow $(1/A)\oint_c k\mathbf{V}\cdot\mathbf{n}ds$ at 0000 GMT. See legend of Fig. 1 for description of curves

5.5-day ($f=22$) and 2.9-day ($f=42$) periods also exceed the 5% significance level although they are not as obvious as the 4-day period.

Fig. 2 is the time spectra of $\bar{k}$ at 1200 GMT. The trend of the high resolution time spectrum at this time of observation is quite the same as that of the 0000 GMT observations with the 40-day period still being dominant. However, instead of the 19-day significant period in the 0000 GMT observations, it has a 7.5-day ($F=48$) period just over the 5% significance level. This 7.5-day period also can be found in the low resolution spectrum. Another important feature in the low resolution spectrum is the broad and high peak around the 3-day ($f=40$) period. Comparing the time spectra of $\bar{k}$ at 0000 and 1200 GMT observations, both have definite 40-day cycles. As for the higher frequency range, the spectrum of 12 GMT observations tends to have cycles of a little shorter period than that of 0000 GMT observations.

The time spectra of $-\overline{\mathbf{V}\cdot\nabla\phi}$ at 0000 GMT is shown in Fig. 3. In the high resolution spectrum, no important period can be found. However, maxima without statistical significance at frequencies of 10, 22, 31 and 51 may be observed. Although the 1-year and half-year cycles have been removed before time spectrum analysis, periods >1 year could add their effect to the first frequency in that time spectrum. Applying the direct harmonic analysis (Kung and Soong, 1969) to the monthly mean value of $-\overline{\mathbf{V}\cdot\nabla\phi}$ averaged for 0000 and 1200 GMT observations over this 5-year period, it is found that the fractional variance of the 5-year period which may be due to cycles >5 years is 13.2%. This is one-third of the fractional variance of the 1-year cycle and about twice as large as that of the half-year cycle. As for the low resolution time spectrum, there is a significant period at 2.3 days ($f=53$). The spectrum is no more than a red noise property at other frequencies.

Fig. 4 is the time spectra of $-\overline{\mathbf{V}\cdot\nabla\phi}$ at 1200 GMT. It has a high fluctuation around the red noise spectrum in comparison with that of the 0000 GMT observations, although some of the maxima of the time spectra at 0000 and 1200 GMT are coincident in both the high and low resolution spectra. In the high resolution spectrum, there is a peak at the period of 40 days ($F=9$) over the 1% significance line, while the 23-day ($F=16$) period also seems significant. The low resolution time spectrum shows a significant period of 2.3 days ($f=53$) which is also evident in the spectrum at 0000 GMT. The significance of the periods at 3.2 days ($f=37$) falls between 5% and 1%.

Fig. 5 contains the time spectra of $(1/A)\oint_c k\mathbf{V}\cdot\mathbf{n}ds$ at 0000 GMT. The high resolution spectrum has an important period around 36 days ($F=10$) which is over

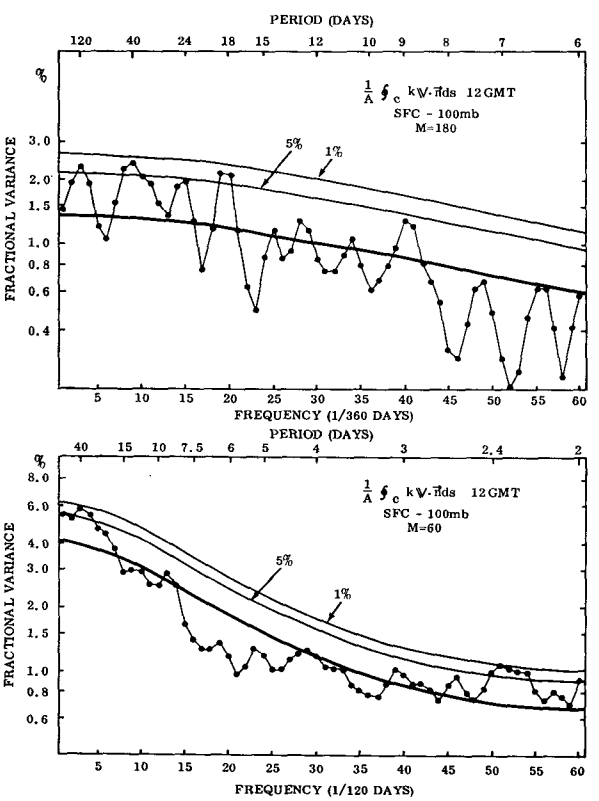


FIG. 6. Same as Fig. 5 except for 1200 GMT.

TABLE 2. Per cent variance of unsmoothed time spectra of kinetic energy $\bar{k}$ at 0000 GMT for each year from May 1958 to April 1963. The basic period is 120 days ($M=60$), $f$ is the frequency, and $P$ the period in days.

| $f$ | $P$ | 1958–59 | 1959–60 | 1960–61 | 1961–62 | 1962–63 |
|---|---|---|---|---|---|---|
| 1 | 120.0 | 12.2 | 7.0 | 10.1 | 6.7 | 8.5 |
| 2 | 60.0 | 13.6 | 8.0 | 6.7 | 2.9 | 10.7 |
| 3 | 40.0 | 0.7 | 15.6 | 20.0 | 30.8 | 20.6 |
| 4 | 30.0 | 6.0 | 5.9 | 7.7 | 3.5 | 11.8 |
| 5 | 24.0 | 0.3 | 8.3 | 4.3 | 2.4 | 0.7 |
| 6 | 20.0 | 9.7 | 6.6 | 5.7 | 9.3 | 12.4 |
| 7 | 17.1 | 6.5 | 2.6 | 3.3 | 4.2 | 8.5 |
| 8 | 15.0 | 8.6 | 2.6 | 2.8 | 7.2 | 2.0 |
| 9 | 13.3 | 8.4 | 1.9 | 4.0 | 2.8 | 1.3 |
| 10 | 12.0 | 1.1 | 6.8 | 3.5 | 0.1 | 0.6 |
| 11 | 10.9 | 1.0 | 2.9 | 4.8 | 3.1 | 2.6 |
| 12 | 10.0 | 3.9 | 3.0 | 0.0 | 0.3 | 1.1 |
| 13 | 9.2 | 4.5 | 1.2 | 3.0 | 4.8 | 1.0 |
| 14 | 8.6 | 0.6 | 1.8 | 2.5 | 1.3 | 0.6 |
| 15 | 8.0 | 1.8 | 1.1 | 0.5 | 1.3 | 0.5 |
| 16 | 7.5 | 0.0 | 1.8 | 1.9 | 2.0 | 1.6 |
| 17 | 7.1 | 0.9 | 0.7 | 0.8 | 1.4 | 1.4 |
| 18 | 6.7 | 0.3 | 0.7 | 0.7 | 1.8 | 0.1 |
| 19 | 6.3 | 2.1 | 0.8 | 2.1 | 0.0 | 1.0 |
| 20 | 6.0 | 0.1 | 0.7 | 0.7 | 1.2 | 0.6 |
| 21 | 5.7 | 0.7 | 1.1 | 0.9 | 1.2 | 0.5 |
| 22 | 5.5 | 1.9 | 2.4 | 2.1 | 0.1 | 1.1 |
| 23 | 5.2 | 1.0 | 0.1 | 0.6 | 1.3 | 0.5 |
| 24 | 5.0 | 0.9 | 0.5 | 0.2 | 1.4 | 0.4 |
| 25 | 4.8 | 0.3 | 1.0 | 0.1 | 0.2 | 0.4 |
| 26 | 4.6 | 0.3 | 0.4 | 0.8 | 0.5 | 0.5 |
| 27 | 4.4 | 0.7 | 0.3 | 0.4 | 0.6 | 0.8 |
| 28 | 4.3 | 0.1 | 0.8 | 0.3 | 0.5 | 0.0 |
| 29 | 4.1 | 0.4 | 0.0 | 0.2 | 0.3 | 0.6 |
| 30 | 4.0 | 0.2 | 0.9 | 0.3 | 0.8 | 1.1 |
| 31 | 3.9 | 0.4 | 1.6 | 0.0 | 0.3 | 0.1 |
| 32 | 3.8 | 0.5 | 0.9 | 1.1 | 0.1 | 0.4 |
| 33 | 3.6 | 0.6 | 0.4 | 0.3 | 0.3 | 0.5 |
| 34 | 3.5 | 0.1 | 0.7 | 1.0 | 0.2 | 0.3 |
| 35 | 3.4 | 0.8 | 0.0 | 0.1 | 0.4 | 0.3 |
| 36 | 3.3 | 0.6 | 0.5 | 0.4 | 0.3 | 0.0 |
| 37 | 3.2 | 0.6 | 0.0 | 0.0 | 0.4 | 0.3 |
| 38 | 3.2 | 0.1 | 0.5 | 0.3 | 0.2 | 0.2 |
| 39 | 3.1 | 0.2 | 0.2 | 0.4 | 0.2 | 0.1 |
| 40 | 3.0 | 0.4 | 0.8 | 0.4 | 0.1 | 0.0 |

the 1% significance line. The 19-day ($F=19$) period falls just at the 5% line. No important period shows in other portions. The low resolution spectrum displays relative important periods of less than 2.6 days, among which the period at 2.5 days ($f=48$) seems to be the most significant.

Fig. 6 shows significant periods of $(1/A)\oint_c k\mathbf{V}\cdot\mathbf{n}ds$ at 1200 GMT of 40 days ($F=9$) and 19 days ($F=19$) in the high resolution spectrum. In the low resolution spectrum, the periods around 2.4 days ($f=51$) look more important.

In general, the time spectra at 0000 and 1200 GMT observations have the same trend with slight differences in the fractional variance of corresponding maxima. The correspondence between the $-\overline{\mathbf{V}\cdot\nabla\phi}$ and $(1/A)\oint_c k\mathbf{V}\cdot\mathbf{n}ds$ spectra also should be noted.

Although the time spectra of kinetic energy parameters derived from the 5-years' data show some maxima which have statistical significance, they are by no means regular. The same time spectrum analysis was applied to the same kinetic energy parameters for individual years separately for the purpose of examining the year-to-year changes in the time spectra. Due to the limitation of the number of data in a 1-year period, the autocorrelations for the Fourier analysis was truncated at lag $M=60$ days. In order to pinpoint the important periods of each time spectrum, the time spectra were not smoothed by the weighted mean. Every year begins at 1 May and ends on 30 April.

The time spectra of $\bar{k}$ and $-\overline{\mathbf{V}\cdot\nabla\phi}$ from the 0000 and 1200 GMT observations of each year are given in Tables 2–5, the last 20 frequencies not being listed because they are too small to determine their importance. One must keep in mind that the red noise time spectrum is going down as the frequency increases, and the same deviations from the red noise time spectrum have more significance at higher frequencies than that at lower ones. Table 2 shows the yearly variations for $\bar{k}$ for the 0000 GMT observations. The maxima at the 40-day period are distinct in every year except the

TABLE 3. Per cent variance of unsmoothed time spectra of kinetic energy $\bar{k}$ at 1200 GMT for each year from May 1958 to April 1963. The basic period is 120 days ($M=60$), $f$ is the frequency, and $P$ the period in days.

| $f$ | $P$ | 1958–59 | 1959–60 | 1960–61 | 1961–62 | 1962–63 |
|---|---|---|---|---|---|---|
| 1 | 120.0 | 16.5 | 9.5 | 9.4 | 10.8 | 1.4 |
| 2 | 60.0 | 16.3 | 15.0 | 9.4 | 3.9 | 26.2 |
| 3 | 40.0 | 7.6 | 7.4 | 23.5 | 27.7 | 24.6 |
| 4 | 30.0 | 3.0 | 10.7 | 6.8 | 3.0 | 2.6 |
| 5 | 24.0 | 2.6 | 0.8 | 3.5 | 2.2 | 3.5 |
| 6 | 20.0 | 5.1 | 4.5 | 5.4 | 7.5 | 3.6 |
| 7 | 17.1 | 3.6 | 6.7 | 2.3 | 7.0 | 2.6 |
| 8 | 15.0 | 6.2 | 2.0 | 3.0 | 4.0 | 1.8 |
| 9 | 13.3 | 5.6 | 0.2 | 3.1 | 2.4 | 3.6 |
| 10 | 12.0 | 3.2 | 4.4 | 3.9 | 1.3 | 0.6 |
| 11 | 10.9 | 2.9 | 6.3 | 4.0 | 2.8 | 3.4 |
| 12 | 10.0 | 1.2 | 0.9 | 0.3 | 0.7 | 2.9 |
| 13 | 9.2 | 4.0 | 1.6 | 2.1 | 3.7 | 1.9 |
| 14 | 8.6 | 1.6 | 2.3 | 0.8 | 1.0 | 1.3 |
| 15 | 8.0 | 0.7 | 5.6 | 1.1 | 1.4 | 0.4 |
| 16 | 7.5 | 0.6 | 1.6 | 1.9 | 2.6 | 3.1 |
| 17 | 7.1 | 0.6 | 0.5 | 1.4 | 1.1 | 1.6 |
| 18 | 6.7 | 0.9 | 1.0 | 1.2 | 1.9 | 0.0 |
| 19 | 6.3 | 0.6 | 1.1 | 2.0 | 0.1 | 2.1 |
| 20 | 6.0 | 0.7 | 0.2 | 1.2 | 1.1 | 1.1 |
| 21 | 5.7 | 2.1 | 1.9 | 1.4 | 0.6 | 0.3 |
| 22 | 5.5 | 0.9 | 0.3 | 3.0 | 0.6 | 0.5 |
| 23 | 5.2 | 0.8 | 0.4 | 0.9 | 1.4 | 0.1 |
| 24 | 5.0 | 1.2 | 0.5 | 0.2 | 1.8 | 0.1 |
| 25 | 4.8 | 0.7 | 0.5 | 0.4 | 0.8 | 0.0 |
| 26 | 4.6 | 0.3 | 0.2 | 0.9 | 0.3 | 0.4 |
| 27 | 4.4 | 1.2 | 0.7 | 0.1 | 0.2 | 0.6 |
| 28 | 4.3 | 0.5 | 1.1 | 0.3 | 0.3 | 0.2 |
| 29 | 4.1 | 0.2 | 0.6 | 0.2 | 0.8 | 0.3 |
| 30 | 4.0 | 0.0 | 0.2 | 0.3 | 0.3 | 0.1 |
| 31 | 3.9 | 0.1 | 0.2 | 0.1 | 0.2 | 0.3 |
| 32 | 3.8 | 0.3 | 0.2 | 0.1 | 0.1 | 0.2 |
| 33 | 3.6 | 0.3 | 0.3 | 0.2 | 0.3 | 0.6 |
| 34 | 3.5 | 0.1 | 0.4 | 0.7 | 0.6 | 0.1 |
| 35 | 3.4 | 0.6 | 0.1 | 0.5 | 0.0 | 0.5 |
| 36 | 3.3 | 0.2 | 0.2 | 0.0 | 0.1 | 0.2 |
| 37 | 3.2 | 0.0 | 0.2 | 0.1 | 0.0 | 0.6 |
| 38 | 3.2 | 0.4 | 1.2 | 0.3 | 0.3 | 0.1 |
| 39 | 3.1 | 0.7 | 0.4 | 0.4 | 0.2 | 0.3 |
| 40 | 3.0 | 0.7 | 0.4 | 0.3 | 0.1 | 0.8 |

TABLE 4. Per cent variance of unsmoothed time spectra o kinetic energy generation $-\overline{\mathbf{V}\cdot\nabla\phi}$ at 0000 GMT for each year from May 1958 to April 1963. The basic period is 120 days ($M=60$), $f$ is the frequency, and $P$ the period in days.

| $f$ | $P$ | 1958–59 | 1959–60 | 1960–61 | 1961–62 | 1962–63 |
|---|---|---|---|---|---|---|
| 1 | 120.0 | 4.0 | 3.1 | 1.8 | 5.4 | 4.8 |
| 2 | 60.0 | 1.0 | 4.8 | 0.1 | 1.2 | 2.5 |
| 3 | 40.0 | 2.3 | 5.8 | 5.6 | 6.0 | 6.0 |
| 4 | 30.0 | 3.1 | 2.5 | 3.2 | 3.8 | 5.4 |
| 5 | 24.0 | 2.5 | 3.3 | 3.8 | 0.3 | 2.8 |
| 6 | 20.0 | 0.5 | 6.8 | 3.1 | 7.3 | 2.0 |
| 7 | 17.1 | 2.8 | 2.7 | 1.0 | 3.5 | 4.9 |
| 8 | 15.0 | 2.3 | 1.6 | 1.5 | 3.1 | 4.9 |
| 9 | 13.3 | 1.8 | 2.6 | 3.4 | 3.3 | 1.0 |
| 10 | 12.0 | 1.5 | 0.5 | 3.7 | 0.7 | 7.2 |
| 11 | 10.9 | 2.4 | 4.7 | 2.2 | 2.2 | 1.8 |
| 12 | 10.0 | 1.7 | 4.8 | 4.9 | 3.0 | 0.6 |
| 13 | 9.2 | 2.3 | 1.7 | 2.0 | 3.4 | 1.3 |
| 14 | 8.6 | 1.1 | 2.1 | 0.2 | 2.3 | 0.9 |
| 15 | 8.0 | 2.3 | 0.6 | 2.4 | 2.3 | 1.5 |
| 16 | 7.5 | 0.8 | 1.8 | 2.4 | 0.6 | 1.4 |
| 17 | 7.1 | 0.8 | 1.0 | 3.8 | 3.6 | 4.2 |
| 18 | 6.7 | 1.1 | 2.2 | 2.4 | 0.7 | 1.4 |
| 19 | 6.3 | 0.5 | 1.6 | 0.8 | 2.6 | 1.6 |
| 20 | 6.0 | 1.1 | 1.9 | 1.9 | 0.9 | 2.2 |
| 21 | 5.7 | 0.4 | 1.5 | 2.2 | 3.6 | 2.7 |
| 22 | 5.5 | 3.6 | 0.3 | 0.5 | 1.9 | 2.3 |
| 23 | 5.2 | 4.3 | 1.1 | 1.7 | 1.4 | 0.7 |
| 24 | 5.0 | 1.9 | 0.6 | 1.3 | 1.0 | 1.1 |
| 25 | 4.8 | 3.0 | 2.3 | 0.8 | 1.4 | 0.8 |
| 26 | 4.6 | 0.3 | 2.2 | 0.8 | 4.0 | 0.7 |
| 27 | 4.4 | 1.0 | 3.7 | 1.8 | 1.9 | 1.3 |
| 28 | 4.3 | 0.5 | 1.7 | 0.4 | 0.7 | 1.2 |
| 29 | 4.1 | 1.6 | 2.2 | 1.3 | 0.5 | 0.3 |
| 30 | 4.0 | 2.6 | 0.1 | 3.5 | 0.8 | 1.1 |
| 31 | 3.9 | 1.0 | 1.4 | 0.4 | 2.1 | 1.3 |
| 32 | 3.8 | 1.3 | 0.8 | 1.1 | 1.4 | 0.6 |
| 33 | 3.6 | 3.5 | 1.2 | 0.9 | 0.1 | 2.3 |
| 34 | 3.5 | 0.6 | 1.1 | 2.7 | 1.6 | 1.2 |
| 35 | 3.4 | 1.8 | 1.4 | 0.3 | 0.9 | 1.1 |
| 36 | 3.3 | 2.8 | 0.4 | 2.6 | 0.8 | 1.5 |
| 37 | 3.2 | 1.7 | 0.7 | 0.8 | 0.1 | 2.0 |
| 38 | 3.2 | 2.4 | 1.1 | 0.8 | 1.2 | 0.6 |
| 39 | 3.1 | 1.1 | 1.4 | 1.8 | 0.5 | 0.8 |
| 40 | 3.0 | 2.2 | 0.5 | 1.0 | 0.6 | 1.2 |

first one which seems to have cycles of longer periods. We note that a peak around a 4-day period is greater than the other periods in the second, fourth, and fifth years in the high frequency range. The period around 20 days (which may be considered essentially the same as the 19-day period in the high resolution spectra in Figs. 1–6) is important throughout the 5-year period.

The yearly variations of the time spectrum of $\bar{k}$ at 1200 GMT are shown in Table 3. The 40-day period is still important in the last three years, while the second and fifth year tend to have longer cycles around 60 days. The first year may possess a still longer period of oscillations. The 20-day period is generally important except in the second year which has a larger fractional variance around the period of 17 days. The first year has an important period around 15 days. The 3-day period has a significant peak in Fig. 2, but we find the larger fractional variance around the period only in the first and fifth years.

Table 4 is the yearly time spectra of $-\overline{\mathbf{V}\cdot\nabla\phi}$ at 0000 GMT, where the most important peak of each time spectrum is quite different. The 40-day period has a larger fractional variance from the second through the fifth year. The important period around 20 days exists in the second and fourth year. The 12-day period is important in the third and fifth year and the 10-day period in the second and third year. The first year tends to have shorter cycles and the predominant period is 5.2 days.

The yearly time spectra of $-\overline{\mathbf{V}\cdot\nabla\phi}$ at 1200 GMT are shown in Table 5. The 40-day period is important only in the third and fifth year. In the first, second and fifth years, there is a peak around a 24-day period, with another important period varying year to year, which ranges from 10–17 days. A shorter period around 3.2 days is important in the first and fourth years.

## 4. Remarks

Without considering the statistical significance, an interesting feature concerning $-\overline{\mathbf{V}\cdot\nabla\phi}$ and $(1/A)\oint_c k\mathbf{V}\cdot\mathbf{n}ds$ is that in using the 5-years' time series

TABLE 5. Per cent variance of unsmoothed time spectra of kinetic energy generation $-\overline{\mathbf{V}\cdot\nabla\phi}$ at 1200 GMT for each year from May 1958 to April 1963. The basic period is 120 days ($M=60$), $f$ is the frequency, and $P$ the period in days.

| $f$ | $P$ | 1958–59 | 1959–60 | 1960–61 | 1961–62 | 1962–63 |
|---|---|---|---|---|---|---|
| 1 | 120.0 | 7.2 | 4.7 | 1.1 | 5.1 | 4.9 |
| 2 | 60.0 | 1.3 | 1.7 | 2.8 | 1.4 | 2.9 |
| 3 | 40.0 | 1.5 | 2.0 | 5.7 | 2.5 | 12.6 |
| 4 | 30.0 | 3.9 | 1.8 | 1.8 | 2.5 | 0.0 |
| 5 | 24.0 | 5.6 | 5.0 | 3.1 | 3.1 | 5.1 |
| 6 | 20.0 | 2.3 | 1.1 | 3.7 | 3.5 | 1.8 |
| 7 | 17.1 | 1.6 | 6.3 | 2.1 | 4.5 | 1.8 |
| 8 | 15.0 | 6.4 | 2.0 | 2.4 | 0.3 | 5.3 |
| 9 | 13.3 | 3.0 | 3.1 | 5.2 | 5.1 | 0.4 |
| 10 | 12.0 | 0.7 | 5.7 | 4.7 | 1.6 | 5.4 |
| 11 | 10.9 | 1.0 | 2.0 | 5.2 | 1.0 | 1.5 |
| 12 | 10.0 | 0.9 | 4.0 | 1.7 | 1.5 | 0.9 |
| 13 | 9.2 | 1.2 | 0.6 | 1.6 | 1.3 | 2.9 |
| 14 | 8.6 | 2.4 | 1.8 | 0.8 | 2.3 | 0.7 |
| 15 | 8.0 | 0.9 | 0.6 | 1.1 | 4.1 | 1.3 |
| 16 | 7.5 | 2.7 | 2.0 | 0.7 | 4.0 | 1.6 |
| 17 | 7.1 | 1.5 | 2.1 | 2.3 | 3.2 | 2.3 |
| 18 | 6.7 | 1.3 | 2.9 | 0.9 | 2.0 | 1.1 |
| 19 | 6.3 | 1.6 | 0.4 | 2.1 | 0.7 | 0.7 |
| 20 | 6.0 | 1.4 | 2.3 | 2.8 | 1.5 | 0.7 |
| 21 | 5.7 | 1.2 | 3.0 | 1.5 | 1.9 | 2.5 |
| 22 | 5.5 | 3.5 | 0.7 | 1.9 | 1.3 | 0.1 |
| 23 | 5.2 | 1.2 | 0.2 | 1.2 | 0.1 | 1.8 |
| 24 | 5.0 | 0.9 | 2.0 | 2.2 | 0.9 | 1.2 |
| 25 | 4.8 | 1.2 | 1.2 | 0.4 | 0.7 | 0.4 |
| 26 | 4.6 | 2.2 | 0.1 | 1.4 | 0.3 | 0.4 |
| 27 | 4.4 | 0.9 | 1.4 | 2.8 | 0.8 | 2.0 |
| 28 | 4.3 | 1.5 | 0.8 | 1.5 | 1.1 | 2.0 |
| 29 | 4.1 | 3.2 | 1.2 | 0.5 | 1.5 | 1.3 |
| 30 | 4.0 | 0.2 | 1.0 | 1.8 | 1.8 | 1.0 |
| 31 | 3.9 | 1.0 | 1.0 | 1.3 | 1.0 | 1.0 |
| 32 | 3.8 | 1.4 | 0.6 | 1.0 | 2.0 | 2.5 |
| 33 | 3.6 | 3.1 | 0.9 | 0.6 | 1.3 | 2.9 |
| 34 | 3.5 | 0.1 | 1.6 | 1.7 | 1.3 | 2.5 |
| 35 | 3.4 | 1.2 | 2.6 | 2.2 | 0.4 | 1.5 |
| 36 | 3.3 | 0.6 | 1.6 | 0.9 | 1.4 | 2.4 |
| 37 | 3.2 | 3.4 | 0.3 | 1.4 | 4.8 | 2.3 |
| 38 | 3.2 | 0.5 | 0.9 | 0.3 | 1.8 | 0.7 |
| 39 | 3.1 | 1.4 | 1.0 | 1.6 | 1.1 | 2.3 |
| 40 | 3.0 | 1.8 | 1.2 | 0.6 | 1.6 | 0.8 |

TABLE 6. The corresponding maxima in days among $\bar{k}$, $-\overline{\nabla\cdot\nabla\phi}$ and $(1/A)\oint_c k\mathbf{V}\cdot\mathbf{n}ds$, where $F$ is the frequency of the high resolution time spectrum with a basic period of 360 days, and $f$ is the frequency of the low resolution time spectrum with a basic period of 120 days.

| $\bar{k}$ | | $-\overline{\nabla\cdot\nabla\phi}$ | | $(1/A)\oint_c k\mathbf{V}\cdot\mathbf{n}ds$ | |
|---|---|---|---|---|---|
| 00 GMT | 12 GMT | 00 GMT | 12 GMT | 00 GMT | 12 GMT |
| 40** $F=9$ | 40** $F=9$ | 36 $F=10$ | 40** $F=9$ | 36** $F=10$ | 40* $F=9$ |
| | | | 23** $F=16$ | | 24 $F=15$ |
| 19** $F=19$ | 19 $F=19$ | | | 19* $F=19$ | 19* $F=19$ |
| | 11 $F=32$ | 12 $F=31$ | 12 $F=30$ | 12 $F=30$ | |
| 9 $F=39$ | 9 $F=39$ | | | 9 $F=39$ | 9 $F=40$ |
| 7 $F=48$ | 7* $F=48$ | 7 $F=51$ | 7 $F=51$ | 7 $F=49$ | 7 $F=49$ |
| 4.0** $f=30$ | | 4.0 $f=30$ | 4.4 $f=27$ | 4.4 $f=27$ | 4.1 $f=29$ |
| 2.9* $f=42$ | 3.0** $f=40$ | | | 3.0 $f=40$ | 3.1 $f=39$ |
| | | 2.3** $f=53$ | 2.3** $f=53$ | 2.5** $f=48$ | 2.4** $f=51$ |

* Significant at 5% level.
** Significant at 1% level.

both of them have the same maxima around 7-, 4- and 2.4-day periods for both 0000 and 1200 GMT observations; around 36- and 12-day periods for the 0000 GMT observations; and around 40- and 24-day periods for the 1200 GMT observations. The correspondence of maxima in the time spectra of $\bar{k}$ and $(1/A)\oint_c k\mathbf{V}\cdot\mathbf{n}ds$ by both observations around the periods of 40, 19, 9, 7 and 3 days is also obvious, again without considering their statistical significance. The correspondence of maxima among these energy parameters is shown in Table 6 for comparison.

The commonly reported kinetic energy cycles with periods of one to two weeks (see introduction) are observed in our analysis too. However, as discussed in this paper, the confidence level of statistical significance and the year-to-year regularity for the cycles of these periods seems to be rather low. Instead, the longer period cycles of 36–40 days and 19–20 days, and shorter periods of 2–4 days, seem to possess higher statistical significance and more regularity.

*Acknowledgments.* We are grateful to Profs. J. E. Holstein, D. L. Darkow, J. D. McQuigg and Mr. D. H. McInnis for reviewing the original manuscript as well as for stimulating discussions. Special acknowledgment goes to Mrs. B. E. Applegate and Mrs. P. C. Brewer for their technical assistance.

## REFERENCES

Alter, D., 1933: Correlation periodogram investigation of English rainfall. *Mon. Wea. Rev.*, **61**, 345–350.

Blackman, R. B., and J. W. Tukey, 1958: *The Measurement of Power Spectra.* New York, Dover Publ., 190 pp.

Brooks, C. E. P., and M. Carruthers, 1953: *Handbook of Statistical Methods in Meteorology.* London, Her Majesty's Stationery Office, 412 pp.

Fultz, D., R. R. Long, G. V. Owens, W. Bohan, R. Kaylor and J. Weil, 1959: Studies of thermal convection in a rotating cylinder with some implications for large-scale atmospheric motions. *Meteor. Monogr.*, **4**, No. 21, 104 pp.

Gilman, D. L., F. J. Fuglister and J. M. Mitchell, 1963: On the power spectrum of 'Red Noise'. *J. Atmos. Sci.*, **20**, 182–184.

Griffith, H. L., J. A. Panofsky and I. Van der Hoven, 1956: Power spectrum analysis over large ranges of frequency. *J. Meteor.*, **13**, 279–282.

Kung, E. C., 1966: Kinetic energy generation and dissipation in the large-scale atmospheric circulation. *Mon. Wea. Rev.*, **94**, 67–82.

——, 1967: Diurnal and long-term variations of the kinetic energy generation and dissipation for a five-year period. *Mon. Wea. Rev.*, **95**, 593–606.

——, and S. Soong, 1969: Seasonal variation of kinetic energy in the atmosphere. *Quart. J. Roy. Meteor. Soc.*, **95** (in press).

Lorenz, E. N., 1963: The mechanics of vacillation. *J. Atmos. Sci.*, **20**, 448–464.

Panofsky, J. A., and G. W. Brier, 1965: *Some Applications of Statistics to Meteorology.* The Pennsylvania State University Press, 224 pp.

Shapiro, R., and F. Ward, 1960: The time-space spectrum of the geostrophic meridional kinetic energy. *J. Meteor.*, **17**, 621–626.

Smagorinsky, J., 1963: General circulation experiments with primitive equations. *Mon. Wea. Rev.*, **91**, 99–164.

——, S. Manabe and J. L. Holloway, Jr., 1965: Numerical results from a nine-level general circulation model of the atmosphere. *Mon. Wea. Rev.*, **93**, 727–768.

Ward, F., and and R. Shapiro, 1961: Meteorological periodicities. *J. Meteor.*, **18**, 635–656.